



# **MECHANICAL STRUCTURE OPTIMIZATION OF PIPE INSPECTION ROBOT FOR DOMESTIC WATER PIPE LINE**

Khairulnizam Othman<sup>1\*</sup>, M. Naim<sup>1</sup>, M. Iqbal<sup>1</sup>, Naomi<sup>1</sup>, N. Izlynda<sup>1</sup>, Suhairi Ismail<sup>1</sup>

<sup>1</sup>Department of Mechanical Engineering, Centre for Diploma Studies,  
University Tun Hussein Onn Malaysia

86400, Parit Raja, Batu Pahat, Johor, Malaysia

Phone: +607453-8692; Fax: +607453-8660

\*Email: [nizam@uthm.edu.my](mailto:nizam@uthm.edu.my)

## **ABSTRACT**

Mechanical design pipe inspection robot with various pipe diameter adaptability and automatic traction force installing is developed for long distance inspection of main water pipe nondestructive evaluation and health monitoring with different diameter series. On the basis of analyzing the mechanical actions of the adaptation to pipe diameter and traction force installing, the related mechanical models are established, and their control system structure and control strategy are discussed. The experimental results show that the theoretical analysis in this research is valid and the prototype of this robot can work well in actual underground water pipelines. As a mobile carrier for visual inspection and non-destructive testing to monitor block, corrosion, crack, defect, and wall thickness of main water pipelines, its inspection range extended around 1000 m wireless. Design and implementation consists in

combining the capacity of self-moving with that of self-sustaining and the property of low weight and dimension.

**Key words:** Design pipe inspection; various pipe diameter; Traction force installing; Water pipelines.

## INTRODUCTION

Robotics is never end growing engineering field which improve human daily task and increase work efficiency. These specific operations as inspection, maintenance, cleaning etc. are expensive, thus the application of the robots appears to be one of the most attractive solutions (Kim, Sharma, & Iyengar, 2010). The pipelines are the major tools for the transportation of drinkable water, effluent water, fuel oils, sewage and gas. A lot of troubles caused by piping networks aging, corrosion, cracks, and mechanical damages are possible. Major concert on domestic water line is leak due to a damaged water pipe or pipe bursts. This carry out responsibility for fixing it depends on which section of the pipe is damaged. Allocation damage area takes a lot of time, need an effective seek out in finding the area of breakdown. To understand why this might happen we need to first look at how the plumbing in your house connects to the water main in the street as in Figure 1.

Effectuate continuous activities for inspection, maintenance and repair are strongly demanded. The robots with a flexible structure may boast adaptability to the environment, especially to the pipe diameter, with enhanced dexterity, maneuverability, managing time and priorities, capability to operate under hostile conditions (Li et al., 2007). The wheeled robots are the simplest, most energy efficient, and have the best potential for long range. Loading the wheels with springs, robots also offer some advantages in maneuverability with the ability to adapt to in pipe unevenness, move vertically in pipes, and stay stable without slipping in pipes (Lee et al., 2012; Kwon, Suh, & Yi, 2012). These types of robots also have the advantage of easier miniaturization. The key problem in their design and implementation consists in combining the capacity of self-moving with that of self-sustaining and the property of low weight and dimension (Kim et al., 2009; Park, Kim, & Yang, 2009; Sadeghi & Moradi, 2008).

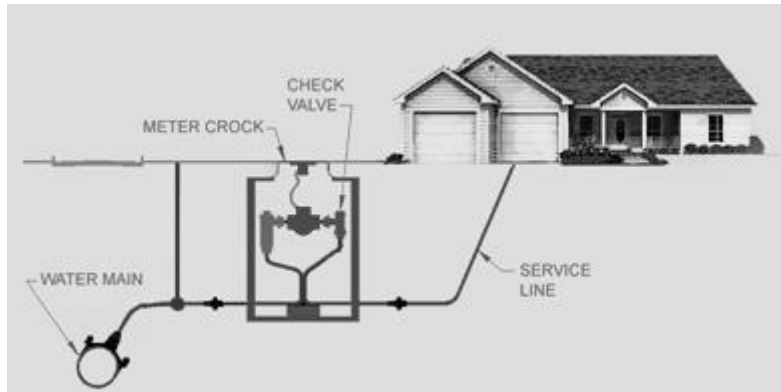


**Figure 1. Water is delivered to house through a service line**

## MODELLING

Its mechanical design employing the scheme that three sets of parallelogram wheeled leg mechanism are circumferentially spaced out  $120^\circ$  apart symmetrically. Each parallelogram wheeled leg has a front driving wheel and a rear driving wheel. Figure 2 illustrates the one of three sets. The operation of the pipe diameter adaptive mechanism is driven by a geared motor with convenience to be controlled. This motor is called the mechanical gear motor. Under the control of motor driver, the motor drives rotation of the gear pair which can push three sets of parallelogram wheeled legs to make driving wheels contact to inner wall of pipe, or adjust the pressure between driving wheels and pipe wall. This structural design makes it possible to realize the adaptability to pipe diameter and traction force installing together, and the pipe diameter adaptive mechanism with this structure can realize adjustment in a wide.

As in Figure 3,  $R$  is the radius of the robot,  $R_1$  is the radius of a pipe,  $h$  denotes the height from the central axis of the inspection robot to supporting point  $D$ ,  $r$  is the radius of a driving wheel,  $L$  is the length of link  $CD$ ,  $L_1$  is the distance between point  $D$  and point  $M$ ,  $L_2$  is the length of link  $MN$ ,  $\alpha$  is the included angles between link  $CD$  and axis  $X$ ,  $\beta$  is the included angles between link  $MN$  and axis  $X$ , and  $F$  denotes the thrust force of mechanism motion, which is caused by the rotation of the gear pair and which can be measured by the pressure sensor. In order to be adaptive for different diameters of pipelines, some bends, and some sections with special shape, the inspection robot needs to change its body size actively. To respond this action, the geared motor drives rotation of the gear with an output torque  $T$  and produces a thrust force  $F$  which can drive translation of parallel linkage  $ABCD$  to change the radial size of the robot, and other two sets of parallelogram wheeled leg perform same action synchronously range.

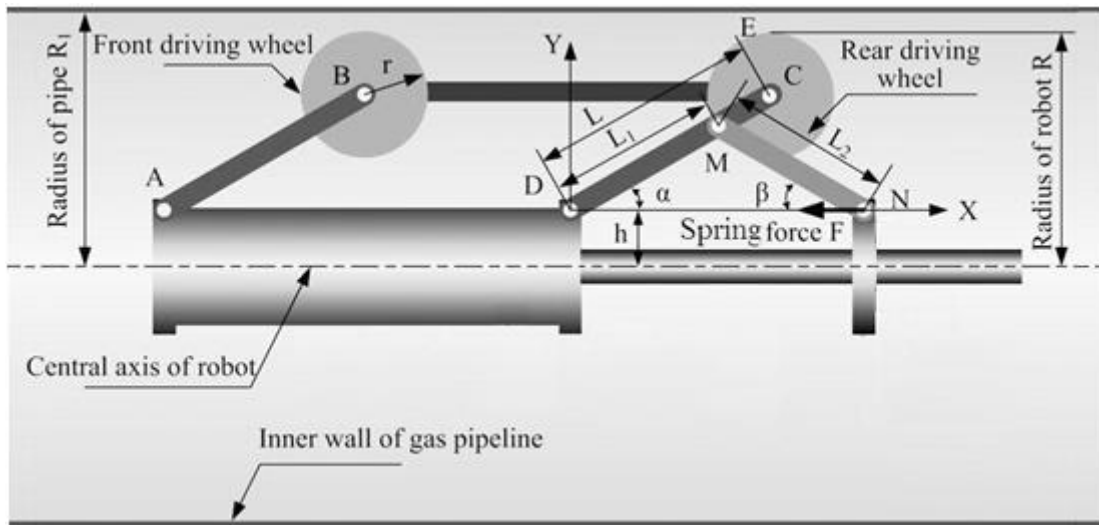


**Figure 2. A various pipe diameter adaptive with wheeled leg mechanism.**

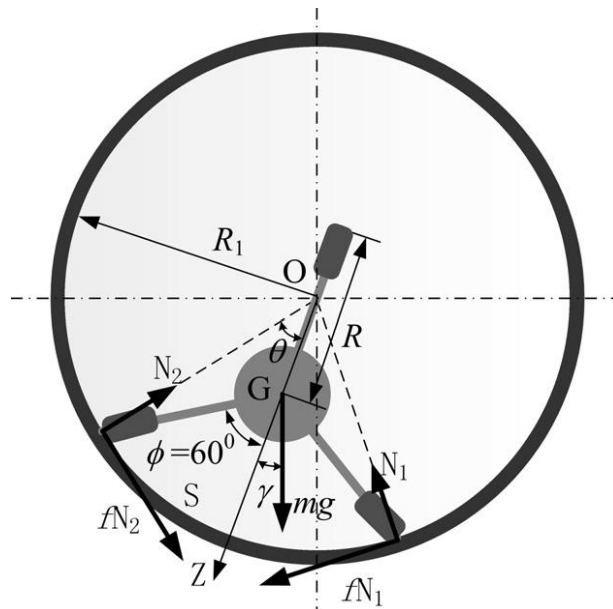


**Figure 3. Robot central axis forced distribution.**

The structure of the robot central axis does not overlap the central axis of pipe as shown in Figure 3, an additional torque is required to overcome the opposition caused by the transverse friction between surface of pipe wall and the wheels supporting the gravity. This may result over loading of the controlled motor. Therefore, we need to analyze this process, and establish its mechanics model to guide the design.

Since the structure of the robot is symmetric, its center of gravity denoted by symbol  $G$  can be assumed at its central axis. In Figure 3, symbol  $\gamma$  denotes the attitude angle of the robot which can reflect its rotation round the central axis of a pipe,  $N_1$  and  $N_2$  respectively denote the

supporting force acting on the two sets of driving wheels by the gravity of the robot,  $\theta$  is the included angle between axis  $OZ$  and the line from the supporting point of a driving wheel to the pipe center,  $s$  is the arc length of  $\theta$ ,  $z$  is the coordinate of  $G$  at axis  $OZ$ , and  $f$  denotes the coefficient of transverse friction between driving wheels and pipe wall. From Figures 3 and 4, we have geometric relationships

$$\begin{aligned}
R &= r + h + L \sin \alpha \\
x &= L_1 \cos \alpha + L_2 \cos \beta \\
L_1 \sin \alpha &= L_2 \sin \beta \\
s &= R_1 \theta \\
R \sin \phi &= R_1 \sin \theta \\
z \sin \phi &= R_1 \sin(\phi - \theta)
\end{aligned} \tag{1}$$

where  $x$  is the coordinate of point  $N$  at axis  $X$ . Differentiating both sides of Eq. (1) yields

$$\begin{aligned}
dx &= -\frac{L_1(R-r-h)}{L} \left( \frac{1}{\sqrt{L^2 - (R-r-h)^2}} + \frac{L_1}{\sqrt{L^2 L_2^2 - L_1^2 (R-r-h)^2}} \right) dR \\
ds &= \frac{R_1 \sin \phi}{\sqrt{R_1^2 - R^2 \sin^2 \phi}} dR \\
dz &= -\left( \cos \phi \frac{R \sin^2 \phi}{\sqrt{R_1^2 - R^2 \sin^2 \phi}} \right) dR
\end{aligned} \tag{2}$$

Ignoring frictional heating, considering a slope angle of pipe, and according to equilibrium equation of forces and conservation of energy, we can obtain

$$\begin{aligned}
\sum N &= N_1 + N_2 = \frac{mg \cos \varphi \cos \gamma}{\cos \theta} = \frac{mg \cos \varphi \cos \gamma R_1}{\sqrt{R_1^2 - R^2 \sin^2 \phi}} \\
Fdx + f \sum Nds &= mgdz \cos \varphi \cos \gamma
\end{aligned} \tag{3}$$

Where  $\sum N$  is the sum of all supporting force.

Defining

$$\sum N = \begin{cases} k_1 = \frac{L_1(R-r-h)}{L} \left( \frac{1}{\sqrt{L^2 - (R-r-h)^2}} + \frac{L_1}{\sqrt{L^2 L_2^2 - L_1^2 (R-r-h)^2}} \right) \\ k_2 = \frac{R_1 \sin \phi}{\sqrt{R_1^2 - R^2 \sin^2 \phi}} \\ k_3 = \cos \phi + \frac{r \sin^2 \phi}{\sqrt{R_1^2 - R^2 \sin^2 \phi}} \\ k_4 = \frac{R_1}{\sqrt{R_1^2 - R^2 \sin^2 \phi}} \end{cases} \quad (4)$$

and substituting Eq. (2) into Eq. (3), we have

$$F = \frac{mg \cos \phi \cos \gamma}{k_1} (k_2 k_4 f + k_3) \quad (5)$$

Then, the output torque of the geared motor can be written as

$$T = \frac{P_h}{2\pi\eta} F \quad (6)$$

where  $\eta$  denotes the transmission efficiency of the gear pair,  $P_h$  denotes the lead of the gear.

When the motion motor of a wheeled robot can produce an enough driving force, its traction force is determined by the adhesion force which depends on the normal pressure and adhesion coefficient between driving wheels and pipe wall. Thus, a wheeled robot with the pipe diameter adaptive mechanism, which can produce an additional normal pressure to change the adhesion force between driving wheels and pipe wall, is capable of adjusting its traction force in a certain range.

Along with the increase of inspection distance in pipeline upward, more traction force of the robot is demanded to overcome increasing friction resistance of the gravity effect, or an additional kinetic resistance caused by pipe slope (Kwon & Yi, 2012). However, when the motion motor of the robot produces more driving force, the adhesion force only contributed by robot weight may be insufficient, and its driving wheels may slip on the surface of pipe wall. Therefore, an additional pressure enhancing adhesion force should be produced by the pipe diameter adaptive mechanism to improve the traction capacity of the robot. This is realized as the way that the action of the geared motor drives rotation of the gear pair with the

output torque  $T$  and produces the thrust force  $F$  which drives parallel linkage  $ABCD$  to press the driving wheels against inner wall of the pipe with an additional pressure.

To realize the control of the adjustment of traction force, we should establish its mechanical model on the basis of analyzing relationships among traction force, additional pressure, thrust force, and output torque of the geared motor. We define the sum of all pressures applied to driving wheels by the robot weight as total supporting force denoted by symbol  $\sum N$ , and the sum of pressures produced by pipe diameter adaptive mechanism actively as additional pressure denoted by symbol  $\sum P$ . As shown in Figure 4, the central axis of the robot nearly overlaps the central axis of the pipe during the adjustment of traction force. Since three sets of parallelogram wheeled legs are circumferentially spaced out  $120^\circ$  apart symmetrically, any attitude angle of the robot will result that only one or two sets of driving wheel at the bottom are contributors which support the gravity of the robot. In Figure 4,  $N_1$ ,  $N_2$ , and  $N_3$  are used to denote the supporting force applied to three sets of driving wheels respectively. We define that an attitude angle along counter-clockwise is positive, and an attitude angle along clockwise is negative. Then we have

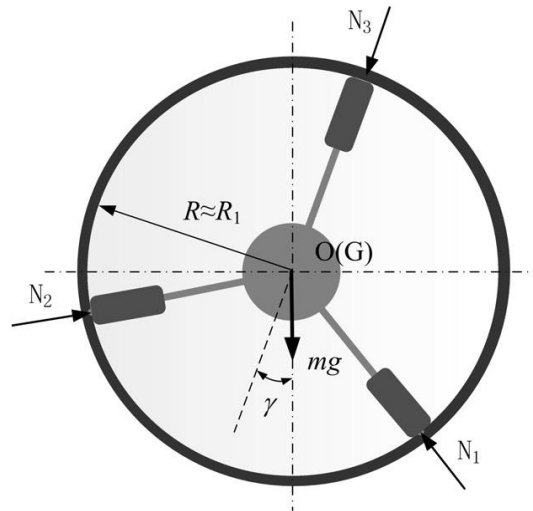


**Figure 4. Real force distribution.**

$$\begin{cases} N_3 = 0 & -60^\circ \leq \gamma \leq 60^\circ \\ N_1 = 0 & 60^\circ \leq \gamma \leq 180^\circ \\ N_2 = 0 & 180^\circ \leq \gamma \leq 300^\circ \end{cases} \quad (7)$$

According to equilibrium of forces, we obtain

$$\begin{cases}
N_1 \cos(\gamma + 60^\circ) + N_2 \cos(60^\circ - \gamma) = mg \\
N_1 \sin(\gamma + 60^\circ) - N_2 \sin(60^\circ - \gamma) = 0
\end{cases} \quad -60^\circ \leq \gamma \leq 60^\circ \\
\begin{cases}
N_2 \cos(\gamma - 60^\circ) - N_3 \cos \gamma = mg \\
N_2 \sin(\gamma - 60^\circ) - N_3 \sin \gamma = 0
\end{cases} \quad 60^\circ \leq \gamma \leq 180^\circ \\
\begin{cases}
-N_3 \cos \gamma + N_1 \cos(60^\circ + \gamma) = mg \\
-N_3 \sin \gamma + N_1 \sin(60^\circ + \gamma) = 0
\end{cases} \quad 180^\circ \leq \gamma \leq 300^\circ
\end{cases} \quad (8)$$

Solving Eq. (8), and considering the slope angle,  $\phi$  we have

$$\sum N \begin{cases}
2mg \cos \gamma \cos \phi & -60^\circ \leq \gamma \leq 60^\circ \\
2mg \cos(\gamma - 120^\circ) \cos \phi & 60^\circ \leq \gamma \leq 180^\circ \\
2mg \cos(\gamma - 240^\circ) \cos \phi & 180^\circ \leq \gamma \leq 300^\circ
\end{cases} \quad (9)$$

If the driving force of the motion motor is sufficient, the traction force of the robot can be written as

$$F_T = (\sum N + \sum P)\mu \quad (10)$$

where  $\mu$  denotes the adhesion coefficient. In Figure 3, we have geometric relationships

$$\begin{cases}
R = r + h + L \sin \alpha \\
y = R - h \\
x = L_1 \cos \alpha + L_2 \cos \beta \\
L_1 \sin \alpha = L_2 \sin \beta
\end{cases} \quad (11)$$

where  $x$  is the coordinate of point  $N$  at axis  $X$ ,  $y$  is the coordinate of point  $E$  at axis  $Y$ .

Differentiating both sides of Eq. (11) yields

$$\begin{cases}
\partial y = \partial R \\
\partial x = k_1 \partial R
\end{cases} \quad (12)$$

Applying principle of virtual displacement yields

$$(\sum N + \sum P)\partial y + F\partial x = 0 \quad (13)$$

Substituting Eq. (12) into Eq. (13), we obtain

$$F = \frac{1}{k_1} (\sum N + \sum P) = \frac{1}{k_1 \mu} F_T \quad (14)$$

Then, the required output torque of geared motor can be written as

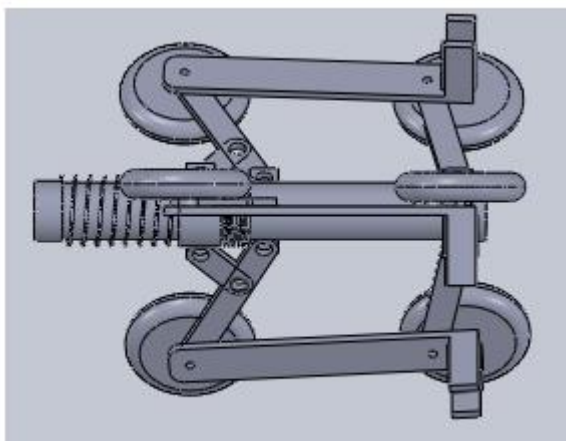


$$T = \frac{P_h}{2\pi\eta} F \quad (15)$$

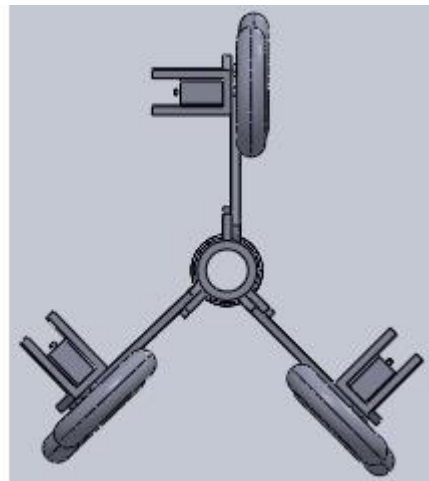
The mechanical model of the traction force employ is composed of Eqs. (9), (10), (14) and (15) which can describe variations of the thrust force  $F$ , output torque  $T$  of the geared motor, additional pressure  $RP$ , and traction force  $FT$  (Kim et al., 2009). When combining the virtual force derived from a potential field which is generated at each wheel module, consider the robot as a point of mass (Takahashi et al., 2011).

## RESULTS AND DISCUSSION

From above mechanical model of dynamic adaptation to pipe diameter, it is known that both the required thrust force  $F$  and the required output torque  $T$  change as  $R_1$  and  $R$  change in the behaviour that the inspection robot adjusts its size to fit variation of pipe diameter, and both  $F$  and  $T$  have different variation in the case of the pipe diameter being different as shown in Figure 5, where  $D = 2R$  and  $D_1 = 2R_1$ . The required  $F$  and  $T$  are more in pipelines with small diameter than in pipelines with large diameter. In order to prevent the geared motor overloading, we place a speed reducer with reduction rate of 10:1 between the geared motor and gear, and verify the strength and rigidity of the related components bearing load.



(a)



(b)

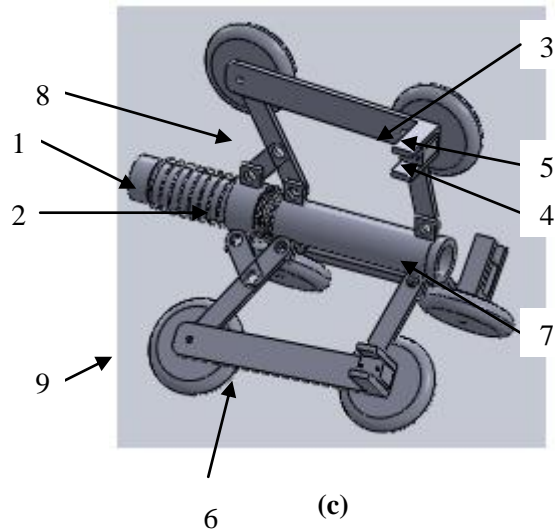


**Figure 5. The 3D model of the pipe inspection robot (a), (b), components of robot (c)**

The force that the robot mechanism exercises on the pipe walls is generated with the help of an extensible spring. The helical spring disposed on the central axis assures the repositioning of the structure, in the case of the pipe diameters' variation. The components of the robot are, (Figure 5, c): 1 - Helical spring, 2 - Translational rings, 3 - Actuator support, 4 - Motor, 5 - Train gear, 6 – link, 7 - Central axis, 8 - Link joint, 9 -Wheel.

In the research, we proposed wheeled type in pipe robots characterized by an adaptable structure based on linkages mechanisms. Compared with the previous research area robots, our prototypes are characterized by a simple structure and kinematics, small number of actuators, light weight, low power consumption. This robot has movement capacities for inspection in 120 - 200 mm diameter pipes in horizontal or vertical configuration.

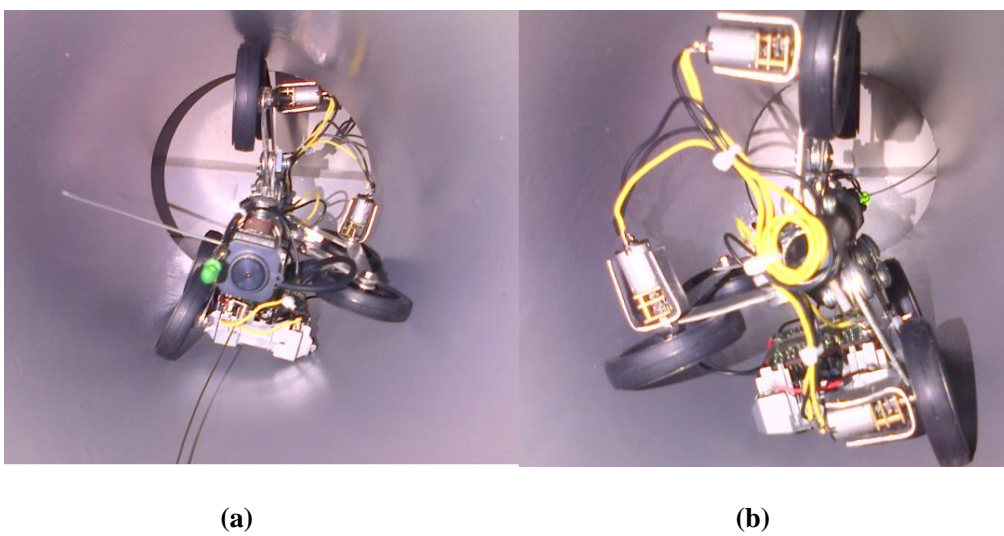


**Figure 6. Picture of the developed in pipe inspection robot**

Elementary mechanism and the structural scheme of the robot is display in Figure 6. The robot is powered through wires and it is controlled with the aid of a microcontroller Microchip PIC18LF4620. The drive DC motors can be powered with the voltage between 2 – 3.5 V. The presented structure used a CCD camera for pipe inspection and sensor devices for malfunction detecting system in pipe inspection (Jero & Ganesh, 2011).

## CONCLUSION

In these research mechanical design pipe inspection robots are proposed. A very important design goal of these robotic systems is the adaptability to the inner diameters of the pipes. Thus, the studied pipe robots are characterized by an adaptable structure, based on linkage mechanisms. The prototypes were designed in order to inspect pipes with variable diameters within 120 and 200 mm which is suitable for water and gas pipeline in urban area. The modular robotic system is development in low power consumption.

## REFERENCES

- [1] Jero, S. E. and Ganesh, A. B. 2011. PIC18LF4620 based customizable wireless sensor node to detect hazardous gas pipeline leakage. *Emerging Trends in Electrical and Computer Technology IEEE Conference*, 1: 563-566.
- [2] Kim, D. W., Park, C. H., Kim, H. K. and Kim, S. B. 2009. Force adjustment of an active pipe inspection robot. *ICCAS-SICE IEEE Conference*, 1: 3792-3797.
- [3] Kim, J. H., Sharma, G. and Iyengar, S. S. 2010. Design concept and motion planning of a single-moduled autonomous pipeline exploration robot. *IECON 2010 -36th Annual Conference on IEEE Industrial Electronics Society*, 1: 1500-1505.
- [4] Kwon, Y. S., Suh, J. T. and Yi, B. J. 2012. A linkage type mechanical clutch synthesis for pipeline inspection robot. *Automation Science and Engineering (CASE), 2012 IEEE International Conference*, 1: 618-623.
- [5] Kwon, Y. S. and Yi, B. J. 2012. Design and Motion Planning of a Two-Module Collaborative Indoor Pipeline Inspection Robot. *Robotics, IEEE Transactions*, 28(3): 681-696.
- [6] Lee, D., Park, J., Hyun, D., Yook, G. and Yang, H. S. 2012. Novel mechanisms and simple locomotion strategies for an in-pipe robot that can inspect various pipe types. *Mechanism and Machine Theory*, 56: 52-68.

- [7] Li, P., Ma, S., Li, B. and Wang, Y. 2007. Development of an adaptive mobile robot for in-pipe inspection task. *Mechatronics and Automation, 2007. ICMA 2007. International Conference*, 1: 3622-3627.
- [8] Park, J., Kim, T. and Yang, H. 2009. Development of an actively adaptable in-pipe robot. In *Mechatronics, 2009. ICM 2009. IEEE International Conference*, 1: 1-5.
- [9] Sadeghi, M. and Moradi, A. 2008. Design and fabrication of a column-climber robot (Koala robot). *Industrial and Aerospace Engineering*, 2: 220-225.
- [10] Takahashi, M., Tada, Y., Suzuki, T. and Yoshida, K. 2011. Hierarchical Action Control Technique Based on Prediction Time for Autonomous Omni-Directional Mobile Robots. *Journal of System Design and Dynamics*, 5(4): 547-559.